Bio-Design and Manufacturing (2022) 5:687–699
https://doi.org/10.1007/s42242-022-00204-4

RESEARCH ARTICLE

Generation of ring-shaped human iPSC-derived functional heart microtissues in a Möbius strip configuration

Yan Xu[1] · Jingqi Qi[2] · Wenyan Zhou[2] · Xing Liu[3] · Longbo Zhang[3,4] · Xudong Yao[5] · Hongwei Wu[1,2]

Received: 17 February 2022 / Accepted: 13 June 2022 / Published online: 26 August 2022

Abstract

Although human-induced pluripotent stem cell-derived cardiomyocytes (hiPSC-CMs) have been used for disease modeling and drug discovery, clinically relevant three-dimensional (3D) functional myocardial microtissues are lacking. Here, we developed a novel ring-shaped cardiac microtissue comprised of chamber-specific tissues to achieve a geometrically non-orientable ventricular myocardial band, similar to a Möbius loop. The ring-shaped cardiac tissue was constructed of hiPSC-CMs and human cardiac fibroblasts (hCFs) through a facile cellular self-assembly approach. It exhibited basic anatomical structure, positive cardiac troponin T (cTnT) immunostaining, regular calcium transients, and cardiac-like mechanical strength. The cardiac rings can be self-assembled and scaled up into various sizes with outstanding stability, suggesting their potential for precise therapy, pathophysiological investigation, and large-scale drug screening.

Graphic abstract

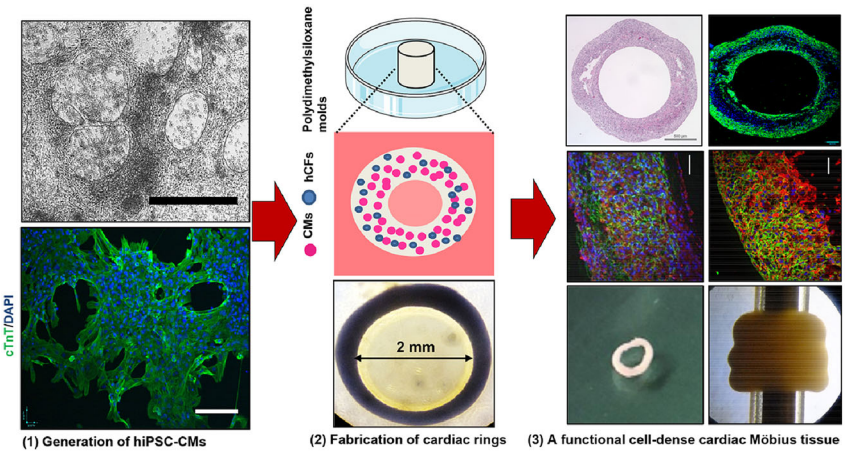

Keywords Human iPSCs · Ring-shaped myocardial microtissue · Ring-shaped cardiac tissue · Myocardial tube

Yan Xu and Jingqi Qi have contributed equally to the work.

✉ Xudong Yao
0617555@zju.edu.cn

✉ Hongwei Wu
wuhongwei@hnca.org.cn

1 Hunan Cancer Hospital and The Affiliated Cancer Hospital of Xiangya School of Medicine, Central South University, Changsha 410013, China

2 Zhejiang University-University of Edinburgh Institute, Haining 314400, China

3 Xiangya Hospital, Central South University, Changsha 410008, China

4 Department of Neurosurgery, School of Medicine, Yale University, New Haven, CT, USA

5 International Institutes of Medicine, The Fourth Affiliated Hospital, Zhejiang University School of Medicine, Yiwu 322000, China

Introduction

Cardiac diseases have multifaceted pathology, in which cellular and acellular players interact to drive the progression [1]. Current cardiac microtissue platforms largely depend on two-dimensional (2D) cell cultures and animal models. Normally, 2D cultures are low-cost and straightforward, but 2D cell culture-based drug-efficacy and toxicity assays fail to predict the cardiomyocyte (CM) response. The in vivo microenvironment and molecular pathways cannot be assessed [2]. On the other hand, animal models may fail to detect the side effects of drugs or mimic disease progression, mainly due to the physiological differences between humans and animals, including beat rate, electrophysiology, myofilament composition, energetics, and calcium cycling [3]. Moreover, ethical and regulatory issues always restrict animal experimentation. Pharmaceutical and biotechnology companies consume extensive resources in drug discovery, but the successful testing rate is only approximately 5% each year [4]. Hence, there is an urgent need to develop novel platforms for understanding cardiac disease progression, disease management, and drug screening.

Three-dimensional (3D) in vitro cardiac models can enhance drug manufacture in terms of the predictability of drug toxicity and sensitivity, since they successfully mimic the tissue architecture with regard to structural organization, cell–extracellular matrix interaction, and cell–cell interaction. The most common types of 3D cell culture are scaffold-based and scaffold-free. Recent advances have applied 3D bioprinters for scaffold-based artificial organ construction by combining biocompatible materials, seed cells, and growth factors [5]. The biomaterials used for cardiac tissue commonly include polycaprolactone [6], sodium alginate [7], and gelatin/methylbenzene sulfonate [8]. Although 3D bioprinting has opened new avenues in mimicking tissue appearance, successful organ construction is not easy to achieve. Moreover, 3D-printing biomaterials present many risks affecting the functions of engineered tissues, including immunogenicity, host inflammatory responses, fibrous tissue formation, material degradation, and toxicity of degradation products [9]. Therefore, scaffold-free tissue engineering, which offers higher cell density, enhanced extracellular matrix (ECM) yield, and greater biocompatibility, is developing rapidly in the areas of regenerative medicine and wound healing [10]. To conclude, scaffold-free tissue engineering offers unprecedented opportunities to generate patient-specific myocardial microtissues with easy, low-cost, and high-efficient procedures.

Cardiac stem cells and their progenitors are promising candidates for cardiac microtissue generation, including embryonic stem cells (ESCs), induced pluripotent stem cells (iPSCs), and somatic stem cells [11]. Autologous somatic stem cells, such as bone-marrow-derived stem cells and adipose-derived stem cells, are free from immune rejection and ethical issues [12]. However, they possess low differentiation potency. ESCs can differentiate into various types of cells, but the ethical issues hamper application for therapeutic treatment. In contrast, iPSCs are a promising source of patient-specific stem cells with high differential potency and less immune rejection or ethical problems [13]. Derivations of iPSCs are minimally invasive using skin biopsy or blood and thus possess a wide range of resources [3]. As iPSCs have strong differentiation capacity, human iPSC-cardiomyocytes (hiPSC-CMs) can be acquired abundantly with CM-like characterizations [3]. Although the first clinical trials with hiPSC derivatives to treat ischemic heart disease showed them to be safe [14], the iPSC-derived functional engineered cardiac tissues for application in humans still possess some technical hurdles, such as immature cardiomyocyte phenotypes, low tissue thickness, and invasive surgical procedures [15]. Novel tissue engineering methods have been employed to promote the functional integrations and long-term viability of engrafted cardiac microtissue [16–18]. At this point, it is vital to demonstrate reproducibility and standardization among various experimental groups for aspects such as cell source, tissue-culture procedures, and platform scalability.

As a revolutionary concept in the 3D architecture of ventricular myocardium, the helical ventricular myocardial band of Torrent-Guasp defines the principal cumulative vectors, tissue structure, and net forces developed within the ventricular mass [19]. To develop a platform for cardiac drug screening, pathological mechanism investigation and heart repair, we constructed a scaffold-free 3D Möbius loop comprising hiPSC-CMs and human cardiac fibroblasts (hCFs) through a facile cellular self-assembly approach. After lactate selection, the hiPSC-CMs showed high purity, which was validated by cardiac troponin T (cTnT) staining. As revealed by type I collagen staining, the cardiac rings showed an appropriate CMs/matrix ratio. Also, they exhibited complete systolic function with the typical electrophysiological characteristics of heart tissue, as measured by the mechanical tests. The cardiac rings can be self-assembled and scaled up into various sizes with outstanding stability, which indicates potential for large-scale and automated applications [20].

Materials and methods

hiPSC differentiation into cardiomyocytes

For this study, hiPSCs generated from human skin fibroblasts were provided by professor Yibing Qyang [21]. Feeder-free cultured hiPSCs were differentiated into CMs, as described

elsewhere [22]. HiPSC clones were washed with phosphate-buffered saline (PBS) once and treated with 1 mg/mL dispase (ThermoFisher) at 37 °C for 7–9 min. The isolated hiPSCs were collected in a 15-mL tube and spun down in a centrifuge. Then they were plated on growth factor reduced matrigel-coated wells (GFR-Matrigel; Corning, 1:60 diluted) for 3–4 days to achieve about 90% confluency. On day 0, the hiPSCs were treated with 20 μM GSK-inhibitor (CHIR99021) for 24 h. Then the medium was changed to RPMI 1640 (Gibco) supplemented with 1% B27 minus insulin (RPMI/B27(−)). On day 3, the medium was switched to RPMI/B27(−) containing 5 μM IWP4 Wnt-inhibitor (Stemgent) for 48 h. RPMI/B27(−) insulin medium was changed every other day during cardiac differentiation. Finally, hiPSC-CMs were cultured with RPMI 1640 supplemented with 1% B27 complete (Gibco). On day 14, hiPSC-CMs were treated with 2 mM lactic acid (Sigma-Aldrich) in sugar-free medium for two days to enrich the hiPSC-CMs and then switched back to RPMI/B27(+) complete medium.

Fabrication of cardiac rings

Custom polydimethylsiloxane (PDMS) molds for cardiac ring fabrication have been presented in another study [23]. We fabricated our cardiac rings with minor modifications [24, 25]. First, 4 mL of 2% autoclaved agarose solution was added into a sterilized PDMS mold with a pipettor. Solidified agarose molds were then stripped from the PDMS mold and equilibrated overnight in RPMI/B27 medium. After that, dispase-dissociated hiPSC-CMs and commercially purchased human cardiac fibroblasts (hCF, ScienCell, #6300) were mixed at a fixed ratio and seeded in RPMI/B27(+) medium at a concentration of 600,000 cells/well. After 24-h culture, cells aggregated into cardiac rings. Two types of ring-culture medium were used to monitor the growth situation and mechanical performance of the cardiac rings. Under the optimized culture conditions, the rings were cultured for a short period (12 days) or mounted on a silicon tube with a diameter of 2 mm for long-term culture (68 days). Then, the rings were harvested and subjected to further mechanical tests and histological analysis. We also twisted cardiac rings into a complex helicoid in vitro, as a demonstration of the Möbius strip configuration.

Cytospin

To detect the purity of the lactate-selected hiPSC-CMs, we performed a cytospin assay. HiPSC-CMs were dissociated with accutase (Sigma-Aldrich) and washed with Dulbecco's phosphate-buffered saline (DPBS). After dissociation, the cells were resuspended to a concentration of 1×10^6 cells/mL in RPMI 1640/B27(+) complete medium. Then, 100 μL of cell suspension was added to the cytospin chamber. The chamber was spun in a cell centrifuge at 400 r/min for 4 min. The slides were then removed and fixed with 4% paraformaldehyde (PFA; Sigma-Aldrich). Cardiac troponin T (cTnT) staining and DAPI staining were performed for the CM purity calculation.

Characterization of cardiac rings

The cardiac rings cultured for different periods of time were washed with DPBS and fixed in 4% PFA at room temperature for 2 h. The rings were divided into three equal parts and sectioned with cryostat (Leica Biosystems) for staining. The morphology of cardiac rings was determined by hematoxylin and eosin (H&E) staining. The phenotypes of the cardiac rings were determined by immunostaining for anti-cardiac troponin T (cTnT, 1:500, Thermofisher, MS-295-P0), α-smooth muscle actin (α-SMA) (1:400, Abcam, AB5694), and collagen I (1:300, Abcam, ab34710).

Immunostaining and histology

The cardiac microtissue sections were boiled at 95 °C in 10 mM citric acid buffer (pH = 6) for 20 min. The sections were then incubated overnight with primary antibody diluted with blocking solution (5% normal goat serum in DPBS) in a 4 °C wet chamber. Sections were washed three times with Tris-buffered saline, incubated for one hour with appropriate secondary antibody diluted 1:500 in blocking solution, and rinsed three times at room temperature. Images were collected using a Nikon 80i microscope and NIS-Elements AR software. Three representative images were taken from three separate slices, and the expression of cTnT, α-SMA, and collagen I was analyzed with ImageJ for semi-quantification statistics.

Contractility assessments

The cardiac rings were carefully removed from the agarose mold and mounted on two hooks in a temperature-controlled perfusion bath. The hooks were connected with two electric micromanipulators with hook-like extensions that allowed the ring to hang between the hooks. There was an anchoring attachment at one end and a force transducer (KG7, SI Heidelberg) at the other (Fig. 4a which will be shown later). Before measurement, the ring was soaked in freshly bubbled Tyrode's solution (NaCl 140 mM, KCl 5.4 mM, $MgCl_2$ 1 mM, HEPES 25 mM, Glucose 10 mM, pH 7.3) containing a gradient concentration of calcium chloride ($CaCl_2$) from 0 to 6 mM. The second reference force was measured 1 mm apart by the manipulator, and the force was measured at the relaxation length. As the cardiac ring's contractile force

changed with the calcium ion concentration, a freshly bubbled Tyrode's solution containing 2.5 mM of $CaCl_2$ was prepared. As mentioned before, the cardiac rings were separated by the manipulator, and this lasted for 15 min. The final change of force was calculated using custom MATLAB software. The PBS-treated rings were then processed to get the baseline value of force change, which was deducted from the initial value of the treatment group to get the final change of force. In addition, we obtained the cross-sectional area of the cardiac ring and calculated the changes in tension (Pa). We evaluated cross sections of tissue rings using optical coherence tomography (Ganymede-II-HR, Thorlabs). The refractive index of each cardiac ring was 1.38. Four images with uniform distance were taken to determine their cross-sectional area with ImageJ, and the average values of the overall cross-sectional area of cardiac ring were calculated.

Mechanical measurements

Before the mechanical test, the ring was removed from the column, and edge-detection software (Framework, DVT) was placed at four different locations around the rings; the average value was taken as the final thickness. The ring was then mounted on a custom grip using a uniaxial tensile testing machine (Electropuls E1000, Instron). The rings were loaded with 5 mN tare, pre-cycled eight times from 5 to 50 mN, and pulled to failure at a speed of 10 mm/min. Finally, the ultimate tensile strength (UTS) and maximum tangent modulus (MTM) were calculated with the custom MATLAB program (The MathWorks Inc.).

Statistics

All testes were repeated two or three times, and there were at least three biological replicates. The P values, determined by the unpaired two-tailed Student's T test and one-way ANOVA, are shown in the figures as $^{*}P < 0.05$, $^{**}P < 0.01$, and $^{***}P < 0.001$.

Results

Optimization of cellular composition in engineered cardiac rings

To mimic the cardiac Möbius strip and reproduce the natural heart structure, we employed a scaffold-free cellular self-assembly approach. First, ventricular cardiomyocytes were reprogrammed with GSK-inhibitor (CHIR99021) from hiPSCs. The selected hiPSC clones showed a typical phenotype indistinguishable from hESCs (Fig. 1a). On day 3 of differentiation, Wnt-inhibitor IWP4 (which determines the efficiency and purity of derived cardiac troponin T (cTnT)-positive CMs) was added into the hiPSC culture (Fig. 1a). To obtain high CM purity, a metabolic selection of lactate was applied. 2 and 4 mM concentrations of lactate showed similar purification rates to iPSC-CMs (Fig. S1 in Supplementary Information). Thus, we changed the medium to B27 medium supplemented with 2 mM lactate for 4 days to purify the hiPSC-CMs. As a result, the lactate selection group produced more cTnT-positive CMs than the non-selective culture system (Fig. 1b). The semi-quantification statistics showed that the hiPSC-CMs took up over 90% of the resulting cells after lactate selection (Fig. 1b). In the electrophysiological test, hiPSC-CMs had similar Ca^{2+} transients (F340/F380) to normal cardiac tissue (Fig. 1c). On day 20 of culture, the excitability, automatic rhythm, conductivity, and contractility of CMs were visible (Video S1 in Supplementary Information).

Next, we found that the initial seeding cell concentration of the 4×10^5 cells/well achieved the most regular and neatest rings. Higher cell concentrations resulted in an irregular and loose shape (Fig. S2a in Supplementary Information). Also, purified CMs alone could not maintain a regular ring shape for a long culture period (Fig. S2b in Supplementary Information). Thus, we mixed the hCFs with CMs to improve ring formation, revealing that a neat ring could be formed when the ratio of CMs/CFs was less than 15:1 (Fig. S3a in Supplementary Information). Ratios of both 9:1 and 4:1 could maintain a regular ring shape until day 20 (Figs. S3b and S3c in Supplementary Information). After 10 days of culture, the CMs/CFs = 4:1 rings appeared denser compared to other groups, and could be easily picked up with tweezers (Fig. 2a). Additionally, the force measurement showed that the tension of CMs + CFs rings was significantly higher than that of rings containing CMs alone (Fig. 1e), indicating an appropriate cell composition to construct a cardiac ring.

In addition to cell type and proportion, the ideal culture medium should be considered. According to the collagen staining of hCFs, the supplement of ascorbic acid and ficoll in B27-containing culture medium stimulated collagen deposition in vitro (Fig. S4 in Supplementary Information). Importantly, the RPMI 1640/B27(+) medium supplemented with ficoll and ascorbic acid was found to stimulate hCFs to produce collagen (Fig. S4b in Supplementary Information). Moreover, the cell rings formed more compact tissue rings in the Basal medium supplemented with fetal bovine serum (FBS), ficoll, and ascorbic acid than in unsupplemented Basal medium (Fig. S5 in Supplementary Information). Ultimately, we selected CMs/CFs = 4:1 cultured in B27 supplemented with FBS, ficoll, and ascorbic acid media as optimized cell-ring culture conditions.

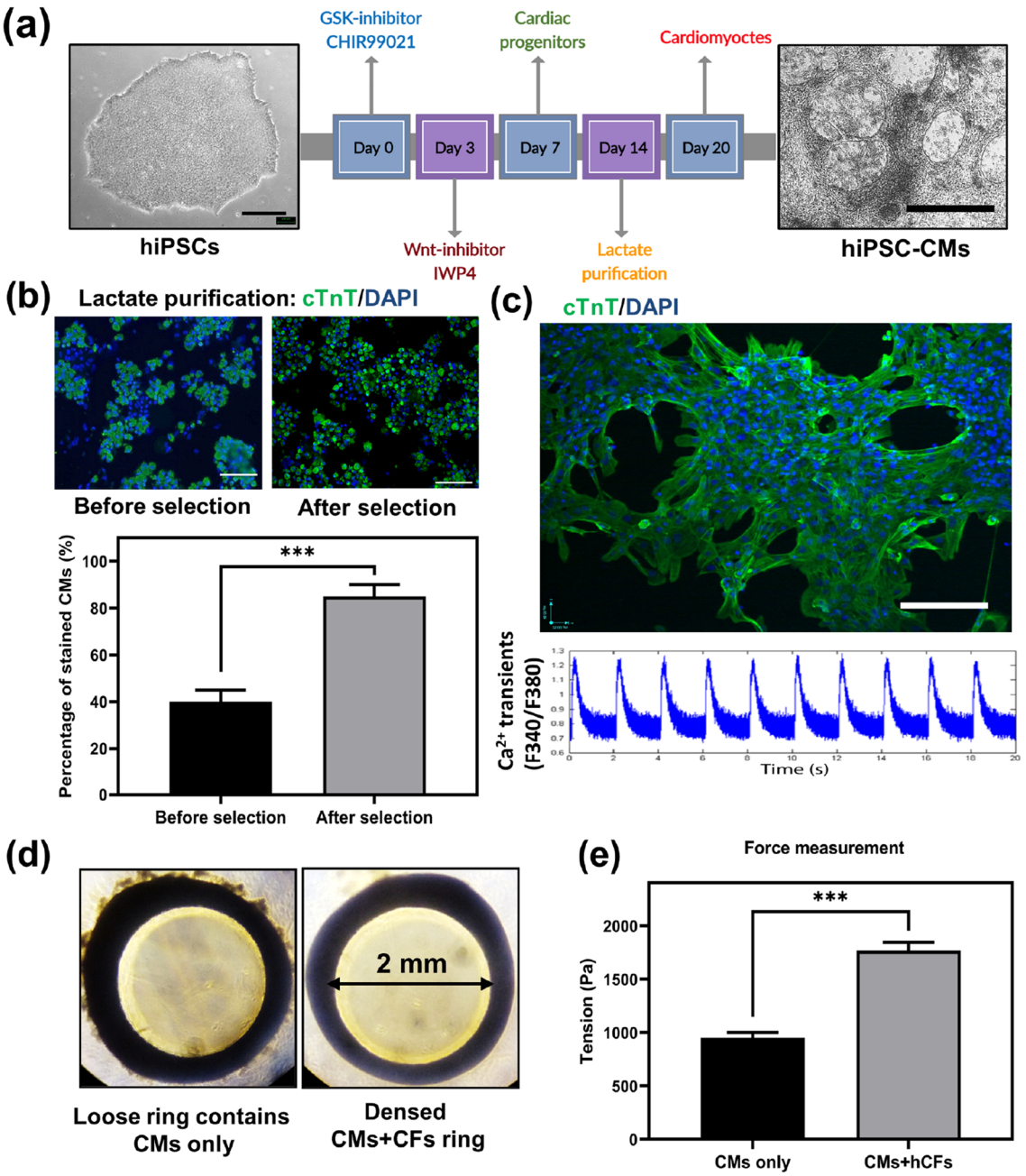

Fig. 1 Optimization of cardiac cellular compositions. **a** hiPSCs differentiated into CMs under the stimulation of GSK-inhibitor, Wnt-inhibitor, and lactate purification. Scale bar: 200 μm. **b** CMs treated with metabolic selection of lactate. Purification efficiency quantified by cTnT intensity. Scale bar: 100 μm. **c** Ca^{2+} transients in hiPSC-CMs. Scale bar: 100 μm. **d** Structural differences between the CMs ring and CMs + CFs ring. **e** Tension difference between the CMs ring and CMs + hCFs ring. Significantly different (one-way ANOVA): $^{***}P < 0.001$

Establishing ring-shaped cardiac tissues

HiPSC-CMs and hCFs were then mixed at a ratio of 4:1 and seeded into ring molds with a diameter of 2 mm (Fig. 2a). Through self-assembly, the 3D architecture of the heart defined by Torrent-Guasp was mimicked successfully. The regular beating of the cardiac ring-shaped myocardial microtissues could be clearly observed on day 6 (Video S2 in Supplementary Information). Under hematoxylin–eosin (H&E) staining of rings, cells were tightly arranged into rings (Fig. 2b). In the cross and longitudinal sections, cells were evenly distributed without necrotic cells (Figs. 2c and 2d).

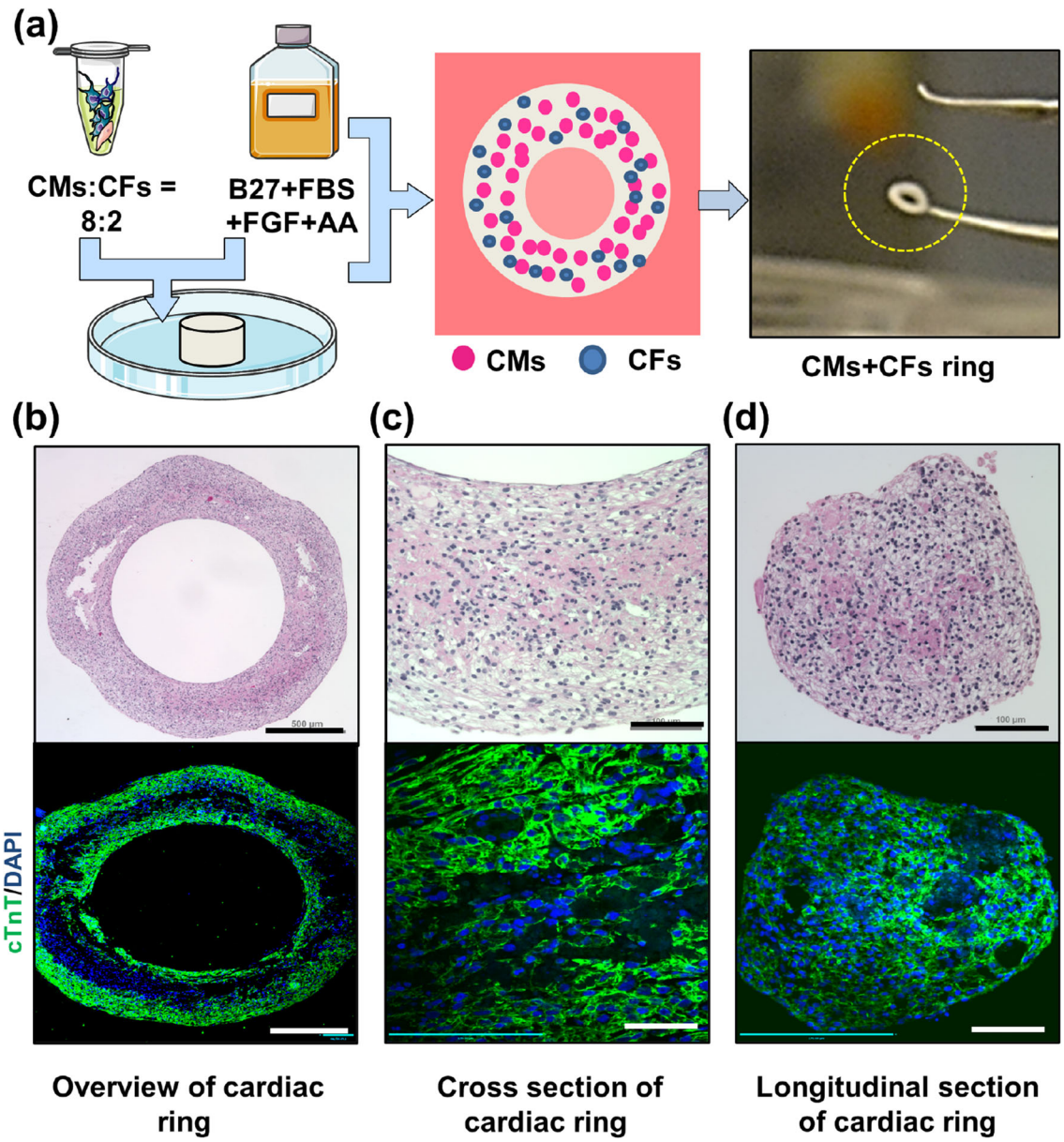

Fig. 2 Generation of ring-shaped cardiac tissue. **a** Schematic illustration of formation of a cardiac ring by culturing CMs with CFs at a cell-number ratio of 4:1. H&E staining and immunofluorescence staining for cTnT of entire cardiac ring (**b**), cross section (**c**), and longitudinal section (**d**). Scale bar: 500 μm (**b**); 100 μm (**c**, **d**)

Immunofluorescence staining manifested high cTnT fluorescence intensity, suggesting that the CMs occupied most of the total cells (Figs. 2b–2d).

Immunohistochemical evaluation

To analyze the cellular distribution of cardiac rings, we performed immunohistochemical analysis using DAPI, cTnT, collagen I, and α-smooth muscle actin (α-SMA) (Figs. 3a and 3b). The rings survived and proliferated for a long time without cell apoptosis, fragmentation, or dissolution, due to significantly higher collagen I relative density on day 68 than day 12 (Fig. 3d). The rings showed higher intensity of cTnT on day 68 than on day 12 (Fig. 3c). Thus, the primary cells constituting the self-assembled and high-density cardiac rings retained a CM phenotype during long-term culture. On both days 12 and 68, cultured rings showed positive α-SMA staining, suggesting that they possessed the characteristics of vascular smooth-muscle cells. This may be due to the differentiation of hiPSC (Fig. 3e). Overall, the cardiac rings successfully mimicked the natural heart structure and were viable for a long time.

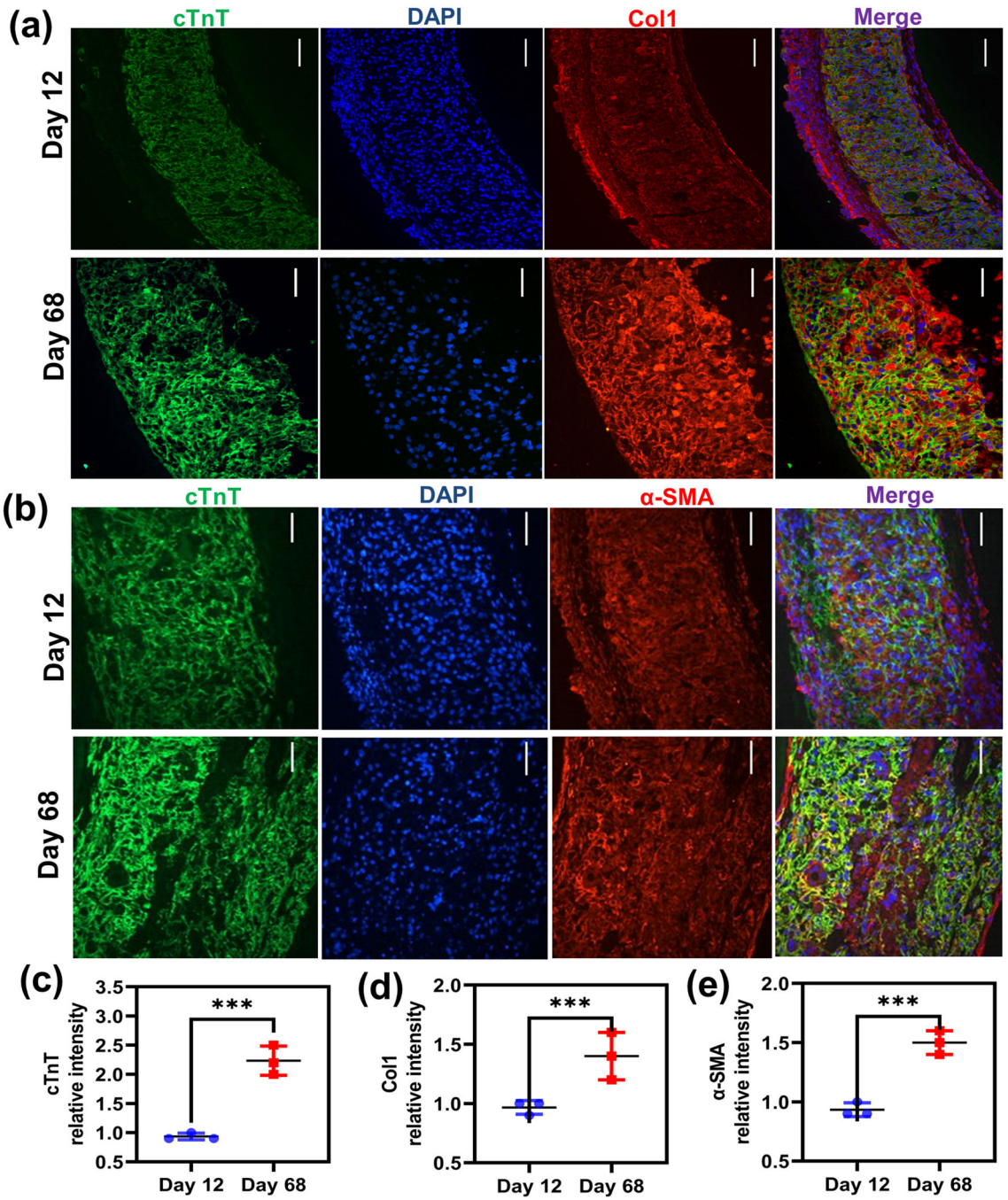

Fig. 3 The long-term maturing of a cardiac ring revealed by immunohistochemical localization from day 12 to day 68 (**a** and **b**) and the corresponding semi-quantification of cTnT expression (**c**), collagen I (**d**), and α-smooth muscle actin (**e**). Significantly different (one-way ANOVA): $^{***}P < 0.001$. Scale bar: 40 μm

Mechanical force determination

The mechanical strength of tissue rings was strong after 20-day culturing (Fig. 4). Four measurements were performed at different locations around the ring circumference and the average thickness of tissue rings with a 2-mm inner diameter was 0.46–0.49 mm. To evaluate the contractile properties, we hung the rings on a device with one pin connected to the force sensor and the other connected to the micromanipulator. The rings generated contractile force in response to 1-Hz electrical impulses (Fig. 4a). Calcium (Ca^{2+}) plays a central role in the excitation–contraction coupling of CMs to regulate electrophysiological processes. The cardiac rings were placed in different solutions containing gradient concentrations of

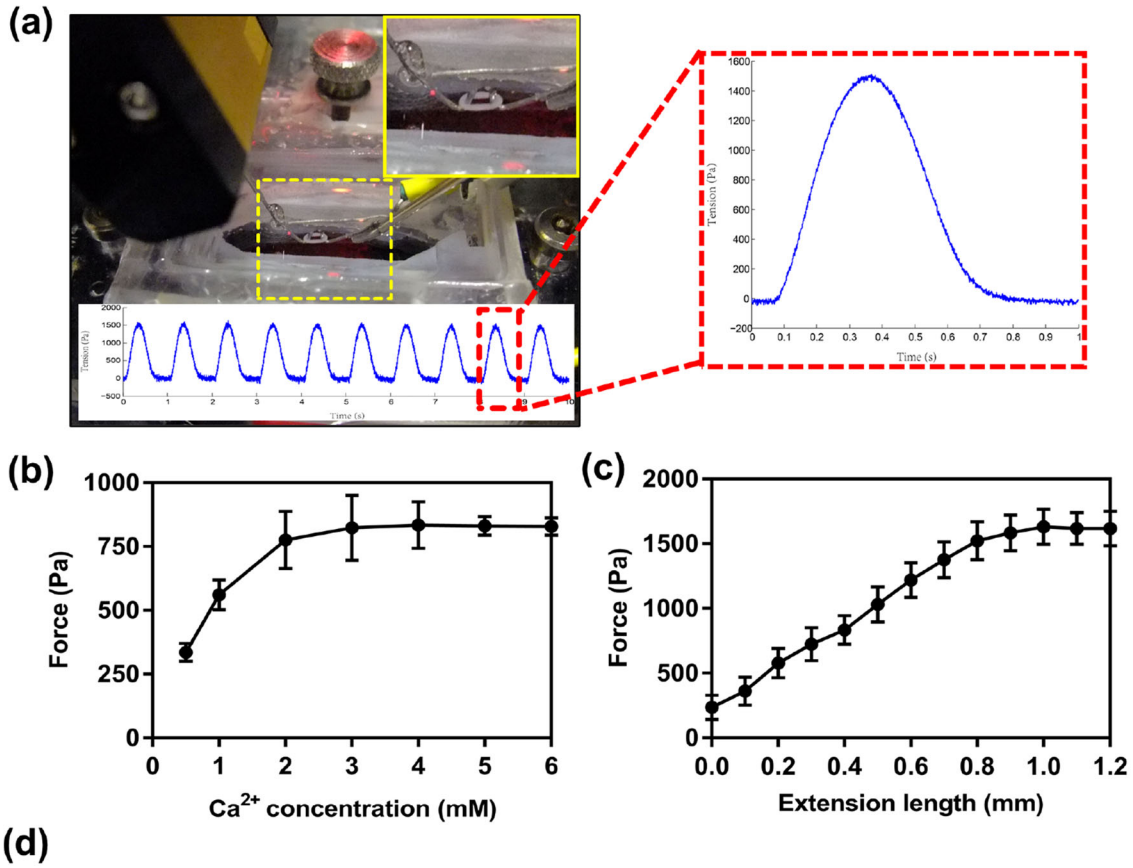

(d)

Ring numbers	Thickness (mm)	UTS (kPa)	MTM (mPa)	Max Strain (mm/mm)	Max Load (mN)	Max Extension (mm)
20	0.46 ± 0.03 0.49 ± 0.03	77.15 ± 7.69 86.12 ± 9.01	0.20±0.02 0.23±0.03	0.56±0.16 0.62±0.06	31.56±4.80 38.79±2.62	1.17±0.24 1.45±0.13

Fig. 4 Mechanical force determination in a cardiac ring. **a** Tracings depicting the contractile force up to 1500 Pa of a cardiac ring over time during sequential stretching in response to electrical impulses. Changes in contractile forces in response to increasing calcium concentration (**b**) and extension length (**c**). **d** Mechanical parameters of cardiac rings, including thickness, ultimate tensile strength (UTS), stiffness (maximum tangent modulus; MTM), failure strain, maximum load, and extension ($n = 20$)

Ca^{2+}, and we found that the 2.5 mM concentration ensured the best electrical impulse propagation and hiPSC-CM ring contraction (Fig. 4b). Then, in the 2.5 mM Ca^{2+} solution, the micromanipulator stretched the ring to increase the force gradually (Fig. 4c). As the extensive length got longer, the force generated from the rings rose rapidly, at a speed of 1.563 kPa/mm, and then changed slowly after 0.8 mm. When the tissue was stretched beyond 50% of its original length, a significantly high force was achieved. Additionally, 20 cardiac rings were used to generate the stress–strain diagrams for UTS and MTM, using a uniaxial tensile testing machine (Electropuls E1000, Instron) (Fig. 4d). The mechanical test data of the cardiac rings are summarized in Fig. 4d. In general, the cardiac rings showed greater UTS than previously reported aortic or human coronary-artery smooth-muscle rings (inner diameter = 2 mm) in 14-day-old rats [25, 26]. The maximum strain was 0.4–0.68 mm/mm, and the maximum load was 26.76–41.41 mN. Additionally, the cardiac rings could be stretched by 0.93–1.58 mm. Similarly to cardiac muscle tissue, the rings possessed good ductility and resistance to pressure.

Constructing large-sized myocardial ring-shaped myocardial tubes

The cardiac ring described here can be considered as a unit tool for constructing a multi-sized cardiac ring-shaped myocardial microtissue (Fig. 5a). A single cardiac ring can

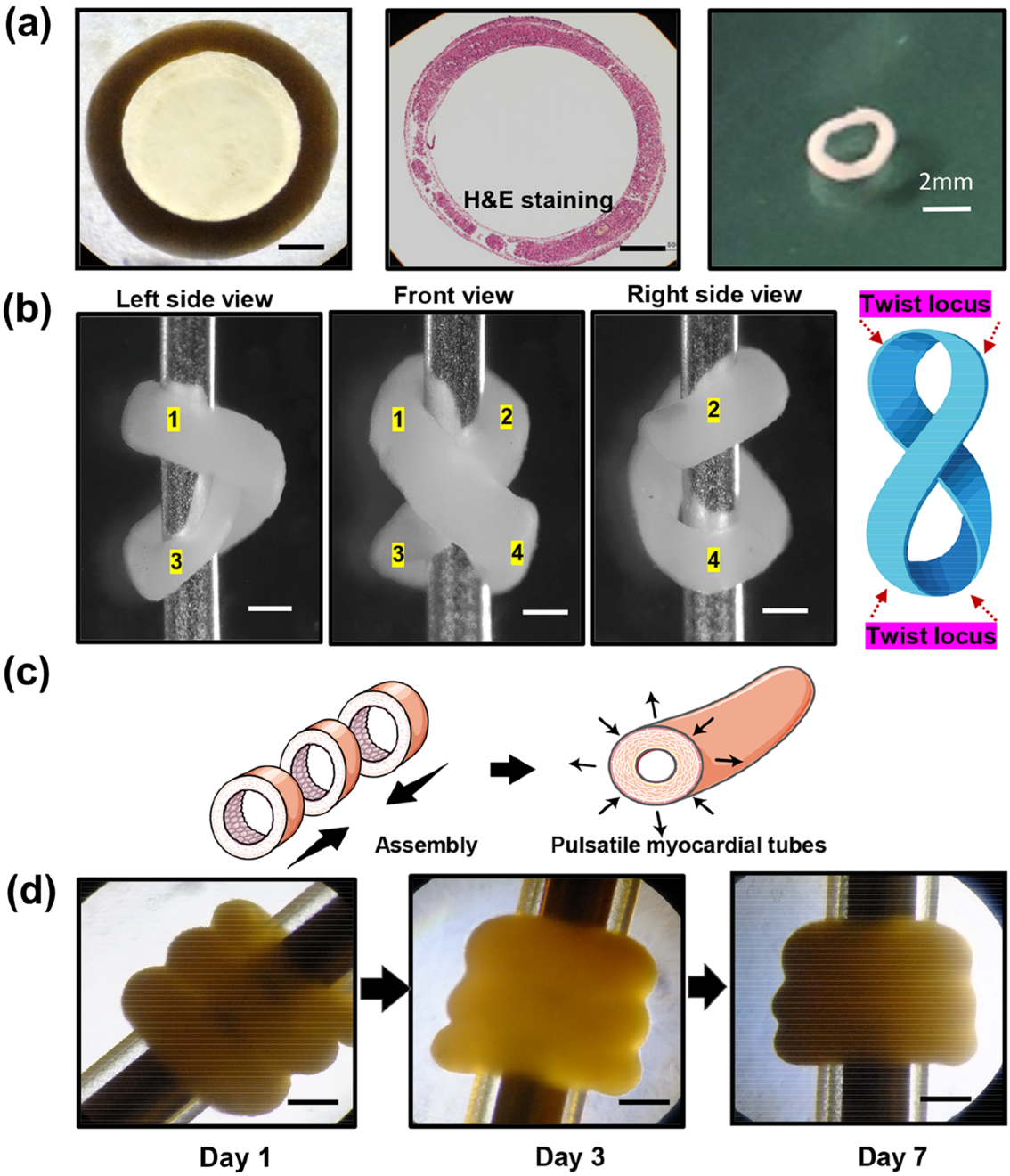

Fig. 5 Construction of large-sized ring-shaped myocardial microtissues. **a** Demonstration of a single cardiac ring. Scale bar in black: 500 μm. **b** Photographs showing the helical cardiac ring with annotated sites of four principal spirals within a complex helicoid: Numbers 1 and 4, left-handed helix; Numbers 2 and 3, right-handed helix. Scale bar in white: 1 mm. **c** Schematic illustration of myocardial tube preparation by assembling three cardiac ring units artificially. **d** Fusion of cardiac rings into a pulsatile myocardial tube for 7-day culture. Scale bar: 1 mm

be reshaped into a complex helicoid comprising both a left-handed and a right-handed helix, showing that 3D architecture could be regarded as a geometrically non-orientable surface similar to a Möbius strip (Fig. 5b). Theoretically, the ring unit could be fused together to make long tube structures and form a functional tissue-engineered pulsatile conduit. Because they produce inner graft pressures, long myocardial tubes may have in vivo potential for circulatory support. In the case of aortic replacement, the host blood flow within the lumen has been stimulated by tube pulsation, showing its ability to enhance thickness with mature myofilaments and elongated sarcomeres [27]. However, this strategy needs to be evaluated by contractile myocardial tube formation via an adaptation of the previously published method [27]. As a proof-of-concept for fabricating our myocardial tubes, we placed three ring units together; they fused together efficiently on day 3, and contracted as a pulsatile myocardial tube (Video S3 in Supplementary Information, Figs. 5c and 5d). On day 7, the gaps between the rings almost disappeared, and the curved outline of each ring's surface became flat and smooth (Fig. 5d). Importantly, the beating and shape of the myocardial tube were maintained as long as 68 days of culture until being harvested for evaluation. Therefore, the cardiac ring units can self-assemble into various-sized cardiac ring-shaped myocardial microtissues.

Discussion

The architecture of the heart has been illustrated by Torrent-Guasp and is regarded as a geometrically non-orientable ventricular myocardial band similar to a Möbius loop [19]. In this study, we successfully constructed a functional cell-dense cardiac tissue through a scaffold-free cellular self-assembly procedure by normalizing cell culture and optimizing cell composition. The resulting rings display engineered mechanical properties with robust elasticity and flexibility (e.g., UTS, MTM and maximum strain) due to abundant ECM synthesis (e.g., collagen I and α-SMA), as illustrated in the graphic abstract. This ring-shaped structure was capable of executing continuous rotation and twisting motions, and we refer to it as a "Möbius ring". Combining hiPSC-CMs and hCFs, the Möbius ring shows cardiac-like characteristics in histological and immunohistochemical analysis, as well as mechanical measurement. Based on the biochemical differences on glucose and lactate metabolism between CMs and non-CMs, lactate selection can yield up to nearly 99% purity of CMs [28]. Also, the high purity of hiPSC-CM has been verified by high expression of cTnT [29], but the cTnT cannot demonstrate the maturation of CMs. Compared with adult CMs, the contractility and mitochondrial functions of immature CMs are insufficient, which may prevent clinical application of hiPSC-CMs in the treatment of heart disease. Collagen type I, a component of the extracellular matrix, plays a vital role in the maturation of CMs and can reflect their growth status [30]. Therefore, we applied both cTnT and collagen type I immunofluorescent staining to detect the growth condition of the cardiac rings. Interestingly, the positive α-SMA staining of cardiac rings indicates that the rings possess mature myofibroblasts which participate in myocardial remodeling [31]. This may be due to the differentiation of hiPSC. To ensure the proper electrical impulse propagation and cardiac contraction, cardiac rings were examined for mechanical force. Abnormal Ca^{2+} regulation may lead to arrhythmia through various mechanisms, including promotion of post-depolarization, ion channel regulation, and structural remodeling [32]. With a proper concentration of Ca^{2+}, the cardiac rings have good contractile force and elasticity. Furthermore, cardiac rings can be cultured for 68 days with functional properties and high stability. Our next long-term experiment will be focused on further verifying suitability for specific applications.

For patients with end-stage heart failure, heart transplantation is the ultimate solution, but it is limited by the relative scarcity of organ donors and complications associated with subsequent immunosuppressive therapy [33]. The goal of myocardial tissue engineering is to create a functional myocardial chamber that can independently pump blood through the circulatory system [34]. Several research groups have made cardiac tubes from cultured cells. A CM suspension has been implanted into a lumen or the outer surface of collagenous tubular scaffolds [35]. Although these studies demonstrate the propagation of electrical signals and morphological similarity to the original myocardium, these cardiac tubes lose significant functions including contractile force or graft internal pressure. The cardiac rings presented here possess similar electrophysiological and mechanical properties to normal myocardium. Moreover, in some studies, CMs have been seeded into biodegradable porous synthetic or natural polymers [36], but the scaffolds may weaken the cellular connections and induce inflammation during biodegradation [33]. Because they combine regenerative medicine and tissue engineering, the scaffold-free cardiac rings can overcome these limitations.

In addition to heart-disease therapies, the cardiac rings can be applied in the treatment of aneurysms. The introduction of endovascular aneurysm repair using stent grafts has revolutionized the field of surgery [37]. Our hiPSC-CM rings can serve as stent grafts of any shape or size, addressing the complex branching between the aortic arch and visceral segments. Since human genome heterogeneity leads to different responses to drugs or treatments, an individualized disease model is vital [38]. Ring-shaped myocardial microtissues

constructed from patient-derived skin fibroblasts and genetically altered iPSCs may address interindividual variability, uncover disease mechanisms, and be applied for drug screenings. Importantly, the cell-ring construction can be scaled up through self-assembling and automatically fusing into a larger size, forming a highly regular and reproducible system. A strongly adhesive hemostatic hydrogel based on biomacromolecules can incorporate rings during clinical implantation [39]. The hydrogel can rapidly undergo gelling after ultraviolet (UV) irradiation and be fixed on the bleeding artery and cardiac wall. The glue has good tolerance and biocompatibility, which promotes tissue adhesion, cell-ring survival, and tissue regeneration. Overall, the cardiac rings have great promise for personalized medicine and discovery of new therapeutics.

Due to the limitations of 2D cell cultures and animal models, human heart-disease modeling and drug discovery face challenges in reproducing cell complexity and animal-to-human transition [1]. Though the hiPSC-CM 2D cell culture models have been designed to study heart disease, including ischemic heart disease [38], they cannot reproduce tissue-specific architecture, diverse functions of multiple cell types participating in disease progression, or in vivo treatment response. As for the animal models, they fail to detect the side effects of drugs or mimic disease progression, due to the physiological differences between humans and animals such as beat rate, electrophysiology, myofilament composition, energetics, and calcium cycling [3]. In addition, ethical and regulatory issues always restrict animal experimentation.

Although adult human heart slices have been reported as an in vitro model for pharmacological trials [40], the lack of organ donors and the low viability of adult cardiac tissues in vitro limit their applications [41]. Recently, hiPSC-derived heart cells have been used as an alternative cell source, with great potential for exploring cardiac pathology and drug discovery, for example familial dilated cardiomyopathy [42]. Additionally, 3D-engineered cardiac ring-shaped myocardial microtissues can mimic in vivo heart physiology such as cell–cell and cell–matrix interactions; but only a few studies have reported cardiac ring-shaped myocardial microtissues with a similar structure to the normal heart. Cardiovascular structures, including vascular structures, cardiac muscle, and heart valve catheters [43], have been constructed through 3D bioprinting, and offer precise structure and functions. However, 3D bioprinting is still in its infancy with regard to generating a heart with full biological functions and complex microstructures. The use of bio-inks, print models, and various print speeds and resolutions may lead to complicated operation, host inflammatory responses, fibrous tissue formation, material degradation, and toxicity of degradation products [9]. In this study, we found that the 3D hiPSC-CMs Möbius cell ring can be easily constructed without a scaffold, achieving rapid and large-scale production.

In this study, CFs were added into the cardiac rings and mixed with hiPSC-CMs at a ratio of 1:4 to mimic heart tissue. This is because CFs are present throughout the myocardium and are enriched in the microenvironment of the ventricular conduction system (VCM). The estimated proportion of CFs to CMs is 0.4–0.7 in the normal human heart [44]. Although CFs/CMs = 1:1 has been used to successfully obtain in vitro cardiac-like tissue [45], the proportion of CFs in cardiac nonmyocytes is reported to be less than 20% [46]. Therefore, to mimic the heart tissue, we chose CMs-CFs at a ratio of 4:1 for our experiments. CFs have also been found to influence the specialization of CMs into ventricular conduction system (VCS) like cells through NOTCH1 signaling [45]. To achieve a more comprehensive organization of heart-ring-shaped myocardial microtissue, various cell types can be simply added into this newly developed Möbius ring in future. Our current work suggests that the structure and function of the cardiac ring gradually mature after 2–3 weeks of culture. Tissue formation can be regulated by biochemical and physical signals. An appropriate dose of Wnt is essential to guide cell fate into the cardiac mesoderm [47]. Otherwise, a lower Wnt signal would cause the formation of endoderm, and a higher Wnt signal would induce differentiation of the precursor mesoderm [24]. To further improve the multiple-cell-ring assembly, various biochemical and biomechanical signals can be considered to build an autonomic and high throughput device to optimize the culture conditions.

In addition to cell type, the arrangement of cells is significant. Although the functional dense cardiac tissue achieved good capabilities, the unidirectional cardiomyocyte alignment, which is significant to generate contractile forces, may be limited by the outer surface of the cardiac rings [48]. Moreover, the circulatory stretching of heart tissue has been proven to promote the longitudinal direction of cells, leading to greater contractile force of tissues [49]. Thus, it is necessary to enhance their contractile properties by mimicking the structure of natural cardiac muscle. The effect of cyclic stretching of cardiac rings on the arrangement and contractility of cardiomyocytes also needs further study.

Conclusions

This paper introduces a facile cellular self-assembly approach to in vitro engineering of heart tissue. The cardiac rings produced show an appropriate CMs/matrix ratio, a high degree of CM differentiation, complete systolic function, outstanding stability, and the typical electrophysiological characteristics of heart tissue. In addition, they have the potential to be scaled up for clinical applications. These miniature myocardial organs can be easily cultured in suspension for at least 68 days. In summary, iPSC-CM-derived

cardiac rings have the potential for miniaturization, automation, and precision medicine.

Supplementary Information The online version contains supplementary material available at https://doi.org/10.1007/s42242-022-00204-4.

Acknowledgements We would like to give special thanks to Prof. Yibing Qyang at Yale University for his scientific suggestions. We appreciate Dr. Yongming Ren for generating human iPS cells and Dr. Ting Yi for contractility and mechanical test. We also appreciate Prof. Stuart Campbell at Yale University and Prof. Marsha W. Rolle at Worcester Polytechnic Institute for their technical support. The study was supported by the Scientific and Technology Platform and Talents Project of Changsha (No. kh1801129) (to HW), Hunan Cancer Hospital Climb Plan (No. YF2020007) (to HW), the Huadong Medicine Joint Funds of the Zhejiang Provincial Natural Science Foundation of China (No. LHDMZ22H020001) (To XY), and the Science and Technology Program of Jinhua Science and Technology Bureau (No. 2021-3-001) (To XY).

Author contributions HW designed the study and performed the mechanical test; YX performed the cell experiments; JQ wrote the manuscript; WZ contributed to experiments related to the second manuscript revision; XL contributed to the statistics analysis; LZ and XY revised the manuscript; XY contributed to the conception of Möbius strip.

Declarations

Conflict of interest The authors declare that they have no conflict of interest.

Ethical approval This study does not contain any studies with human or animal subjects performed by any of the authors.

Data availability The original contributions presented in the study are included in the article and supplementary materials, and further inquiries can be directed to the corresponding authors.

References

1. Goldfracht I, Protze S, Shiti A et al (2020) Generating ring-shaped engineered heart tissues from ventricular and atrial human pluripotent stem cell-derived cardiomyocytes. Nat Commun 11(1):75. https://doi.org/10.1038/s41467-019-13868-x
2. Bissell MJ (2017) Goodbye flat biology—time for the 3rd and the 4th dimensions. J Cell Sci 130(1):3–5. https://doi.org/10.1242/jcs.200550
3. Karakikes I, Ameen M, Termglinchan V et al (2015) Human induced pluripotent stem cell-derived cardiomyocytes: insights into molecular, cellular, and functional phenotypes. Circ Res 117(1):80–88. https://doi.org/10.1161/CIRCRESAHA.117.305365
4. Brancato V, Oliveira JM, Correlo VM et al (2020) Could 3D models of cancer enhance drug screening? Biomaterials 232:119744. https://doi.org/10.1016/j.biomaterials.2019.119744
5. Murphy SV, Atala A (2014) 3D bioprinting of tissues and organs. Nat Biotechnol 32(8):773–785. https://doi.org/10.1038/nbt.2958
6. Yeong WY, Sudarmadji N, Yu HY et al (2010) Porous polycaprolactone scaffold for cardiac tissue engineering fabricated by selective laser sintering. Acta Biomater 6(6):2028–2034. https://doi.org/10.1016/j.actbio.2009.12.033
7. Gaetani R, Doevendans PA, Metz CH et al (2012) Cardiac tissue engineering using tissue printing technology and human cardiac progenitor cells. Biomaterials 33(6):1782–1790. https://doi.org/10.1016/j.biomaterials.2011.11.003
8. Gao L, Kupfer ME, Jung JP et al (2017) Myocardial tissue engineering with cells derived from human-induced pluripotent stem cells and a native-like, high-resolution, 3-dimensionally printed scaffold. Circ Res 120(8):1318–1325. https://doi.org/10.1161/CIRCRESAHA.116.310277
9. Norotte C, Marga FS, Niklason LE et al (2009) Scaffold-free vascular tissue engineering using bioprinting. Biomaterials 30(30):5910–5917. https://doi.org/10.1016/j.biomaterials.2009.06.034
10. Alblawi A, Ranjani AS, Yasmin H et al (2020) Scaffold-free: a developing technique in field of tissue engineering. Comput Methods Programs Biomed 185:105148. https://doi.org/10.1016/j.cmpb.2019.105148
11. Burridge PW, Keller G, Gold JD et al (2012) Production of de novo cardiomyocytes: human pluripotent stem cell differentiation and direct reprogramming. Cell Stem Cell 10(1):16–28. https://doi.org/10.1016/j.stem.2011.12.013
12. Anderson CW, Boardman N, Luo J et al (2017) Stem cells in cardiovascular medicine: the road to regenerative therapies. Curr Cardiol Rep 19(4):34. https://doi.org/10.1007/s11886-017-0841-2
13. Gui L, Dash BC, Luo J et al (2016) Implantable tissue-engineered blood vessels from human induced pluripotent stem cells. Biomaterials 102:120–129. https://doi.org/10.1016/j.biomaterials.2016.06.010
14. Menasché P, Vanneaux V, Hagège A et al (2018) Transplantation of human embryonic stem cell-derived cardiovascular progenitors for severe ischemic left ventricular dysfunction. J Am Coll Cardiol 71(4):429–438. https://doi.org/10.1016/j.jacc.2017.11.047
15. Pomeroy JE, Helfer A, Bursac N (2020) Biomaterializing the promise of cardiac tissue engineering. Biotechnol Adv 42:107353. https://doi.org/10.1016/j.biotechadv.2019.02.009
16. Montgomery M, Ahadian S, Davenport Huyer L et al (2017) Flexible shape-memory scaffold for minimally invasive delivery of functional tissues. Nat Mater 16(10):1038–1046. https://doi.org/10.1038/nmat4956
17. Nguyen HX, Kirkton RD, Bursac N (2018) Generation and customization of biosynthetic excitable tissues for electrophysiological studies and cell-based therapies. Nat Protoc 13(5):927–945. https://doi.org/10.1038/nprot.2018.016
18. Zhang B, Montgomery M, Chamberlain MD et al (2016) Biodegradable scaffold with built-in vasculature for organ-on-a-chip engineering and direct surgical anastomosis. Nat Mater 15(6):669–678. https://doi.org/10.1038/nmat4570
19. Kocica MJ, Corno AF, Carreras-Costa F et al (2006) The helical ventricular myocardial band: global, three-dimensional, functional architecture of the ventricular myocardium. Eur J Cardiothorac Surg 29(Suppl 1):S21–S40. https://doi.org/10.1016/j.ejcts.2006.03.011

20. Nycz CJ, Strobel HA, Suqui K et al (2019) A method for high-throughput robotic assembly of three-dimensional vascular tissue. Tissue Eng Part A 25(17–18):1251–1260. https://doi.org/10.1089/ten.tea.2018.0288
21. Dash BC, Levi K, Schwan J et al (2016) Tissue-engineered vascular rings from human iPSC-derived smooth muscle cells. Stem Cell Rep 7(1):19–28. https://doi.org/10.1016/j.stemcr.2016.05.004
22. Park J, Anderson CW, Sewanan LR et al (2020) Modular design of a tissue engineered pulsatile conduit using human induced pluripotent stem cell-derived cardiomyocytes. Acta Biomater 102:220–230. https://doi.org/10.1016/j.actbio.2019.10.019
23. Adebayo O, Hookway TA, Hu JZ et al (2013) Self-assembled smooth muscle cell tissue rings exhibit greater tensile strength than cell-seeded fibrin or collagen gel rings. J Biomed Mater Res A 101(2):428–437. https://doi.org/10.1002/jbm.a.34341
24. Zhao M, Tang Y, Zhou Y et al (2019) Deciphering role of Wnt signalling in cardiac mesoderm and cardiomyocyte differentiation from human iPSCs: four-dimensional control of Wnt pathway for hiPSC-CMs differentiation. Sci Rep 9(1):19389. https://doi.org/10.1038/s41598-019-55620-x
25. Gwyther TA, Hu JZ, Billiar KL et al (2011) Directed cellular self-assembly to fabricate cell-derived tissue rings for biomechanical analysis and tissue engineering. J Vis Exp 2011(57):e3366. https://doi.org/10.3791/3366
26. Gwyther TA, Hu JZ, Christakis AG et al (2011) Engineered vascular tissue fabricated from aggregated smooth muscle cells. Cells Tissues Organs 194(1):13–24. https://doi.org/10.1159/000322554
27. Mathur A, Loskill P, Shao K et al (2015) Human iPSC-based cardiac microphysiological system for drug screening applications. Sci Rep 5:8883. https://doi.org/10.1038/srep08883
28. Tohyama S, Hattori F, Sano M et al (2013) Distinct metabolic flow enables large-scale purification of mouse and human pluripotent stem cell-derived cardiomyocytes. Cell Stem Cell 12(1):127–137. https://doi.org/10.1016/j.stem.2012.09.013
29. Garbern JC, Helman A, Sereda R et al (2020) Inhibition of mTOR signaling enhances maturation of cardiomyocytes derived from human-induced pluripotent stem cells via p53-induced quiescence. Circulation 141(4):285–300. https://doi.org/10.1161/CIRCULATIONAHA.119.044205
30. Edalat SG, Jang Y, Kim J et al (2019) Collagen type I containing hybrid hydrogel enhances cardiomyocyte maturation in a 3D cardiac model. Polymers 11(4):687. https://doi.org/10.3390/polym11040687
31. Shinde AV, Humeres C, Frangogiannis NG (2017) The role of α-smooth muscle actin in fibroblast-mediated matrix contraction and remodeling. Biochim Biophys Acta Mol Basis Dis 1863(1):298–309. https://doi.org/10.1016/j.bbadis.2016.11.006
32. Sutanto H, Lyon A, Lumens J et al (2020) Cardiomyocyte calcium handling in health and disease: insights from in vitro and in silico studies. Prog Biophys Mol Biol 157:54–75. https://doi.org/10.1016/j.pbiomolbio.2020.02.008
33. Shimizu K, Ito A, Lee JK et al (2007) Construction of multi-layered cardiomyocyte sheets using magnetite nanoparticles and magnetic force. Biotechnol Bioeng 96(4):803–809. https://doi.org/10.1002/bit.21094
34. Zandonella C (2003) Tissue engineering: the beat goes on. Nature 421(6926):884–886. https://doi.org/10.1038/421884a
35. Yost MJ, Baicu CF, Stonerock CE et al (2004) A novel tubular scaffold for cardiovascular tissue engineering. Tissue Eng 10(1–2):273–284. https://doi.org/10.1089/107632704322791916
36. Papadaki M, Bursac N, Langer R et al (2001) Tissue engineering of functional cardiac muscle: molecular, structural, and electrophysiological studies. Am J Physiol Heart Circ Physiol 280(1):H168–H178. https://doi.org/10.1152/ajpheart.2001.280.1.H168
37. Swerdlow NJ, Wu WW, Schermerhorn ML (2019) Open and endovascular management of aortic aneurysms. Circ Res 124(4):647–661. https://doi.org/10.1161/CIRCRESAHA.118.313186
38. Liu Y, Liang Y, Wang M et al (2020) Model of ischemic heart disease and video-based comparison of cardiomyocyte contraction using hiPSC-derived cardiomyocytes. J Vis Exp 2020(159):e61104. https://doi.org/10.3791/61104
39. Hong Y, Zhou F, Hua Y et al (2019) A strongly adhesive hemostatic hydrogel for the repair of arterial and heart bleeds. Nat Commun 10(1):2060. https://doi.org/10.1038/s41467-019-10004-7
40. Camelliti P, Al-Saud SA, Smolenski RT et al (2011) Adult human heart slices are a multicellular system suitable for electrophysiological and pharmacological studies. J Mol Cell Cardiol 51(3):390–398. https://doi.org/10.1016/j.yjmcc.2011.06.018
41. van Amerongen MJ, Engel FB (2008) Features of cardiomyocyte proliferation and its potential for cardiac regeneration. J Cell Mol Med 12(6a):2233–2244. https://doi.org/10.1111/j.1582-4934.2008.00439.x
42. Sun N, Yazawa M, Liu J et al (2012) Patient-specific induced pluripotent stem cells as a model for familial dilated cardiomyopathy. Sci Transl Med 4(130):130ra47. https://doi.org/10.1126/scitranslmed.3003552
43. Cui H, Miao S, Esworthy T et al (2018) 3D bioprinting for cardiovascular regeneration and pharmacology. Adv Drug Deliv Rev 132:252–269. https://doi.org/10.1016/j.addr.2018.07.014
44. Zhou P, Pu WT (2016) Recounting cardiac cellular composition. Circ Res 118(3):368–370. https://doi.org/10.1161/CIRCRESAHA.116.308139
45. da Silva AR, Neri EA, Turaça LT et al (2020) NOTCH1 is critical for fibroblast-mediated induction of cardiomyocyte specialization into ventricular conduction system-like cells in vitro. Sci Rep 10(1):16163. https://doi.org/10.1038/s41598-020-73159-0
46. Pinto AR, Ilinykh A, Ivey MJ et al (2016) Revisiting cardiac cellular composition. Circ Res 118(3):400–409. https://doi.org/10.1161/CIRCRESAHA.115.307778
47. Sung TC, Su HC, Ling QD et al (2020) Efficient differentiation of human pluripotent stem cells into cardiomyocytes on cell sorting thermoresponsive surface. Biomaterials 253:120060. https://doi.org/10.1016/j.biomaterials.2020.120060
48. Akiyama H, Ito A, Sato M et al (2010) Construction of cardiac tissue rings using a magnetic tissue fabrication technique. Int J Mol Sci 11(8):2910–2920. https://doi.org/10.3390/ijms11082910
49. Zimmermann WH, Schneiderbanger K, Schubert P et al (2002) Tissue engineering of a differentiated cardiac muscle construct. Circ Res 90(2):223–230. https://doi.org/10.1161/hh0202.103644